African Scientist Vol. 11, No. 4 December 31, 2010
Printed in Nigeria

1595-6881/2010 $12.00 + 0.00

http://www.klobex.org/afs

AFS 2010154/11406

Kinematic simulation of prey perception in plankton using hydromechanical signals as a means of detection

Saminu Iliyasu Bala

Department of Mathematical Sciences, Bayero University Kano, Nigeria
saminub@yahoo.com, 08035338768

(Received September 27, 2010; Accepted November 6, 2010)

ABSTRACT: When two planktonic microorganisms are in close proximity, the geometry of the surrounding flow field is distorted and this gives rise to hydromechanical disturbances. Copepods can sense these disturbances and utilize them to detect the presence of other microorganisms in the vicinity. In this paper we formulated a kinematic simulation model of prey detection by copepods under small scale turbulence. The results of our analysis have shown that the detection (contact) distance is a dynamic entity rather a fixed number. Furthermore, prey perception depends on relative orientations between predator and prey.

1 Introduction

One can define an encounter (contact) between a planktonic predator and its prey as an event when the two microorganisms move to within a fixed distance (termed the contact radius) from each other [5]. Once they are within this distance, the predator can detect the presence of the prey. The detection technique could be visual, as in fish larvae, or chemical and hydromechanical signals (see [3, 16, 17, 4]). For a visual encounter, explicit geometrical representations of encounter scenarios such as positioning of the perception field (detection region) together with some physical insights into the encounter process allow for the development of encounter rates equations (see [5, 14, 9, 10, 8]).

The encounter scenario for hydromechanical perception does not conform to any specific geometry (see [2]). Experimental and theoretical investigations have shown that the ability to detect and react to hydromechanical signals is well developed in copepods (see [16, 17]). Their first antennae are adorned with array of hair-like setae which are highly sensitive to fluid motion (see [21]) and can sense the flow disturbance generated by other bodies in close proximity (see [17, 18, 21]). Although there exists a lot of evidence in support of the fact that copepods respond behaviourally to hydromechanical signals, it is not very clear which components of the fluid disturbance (fluid velocity, velocity gradient, fluid acceleration) they respond to. [15] reported

that for predators perceiving prey, the relevant signal strength is the absolute magnitude of the velocity.

The aim of this paper is to create a highly simplified model of planktonic encounter rates using hydromechanical signals as a means of detection. The simplest possible analytical model of this scenario is the case of two rigid spheres moving past each other in a viscous incompressible fluid. Using the solution of Stokes equations in bispherical coordinates and Kinematic simulation, a novel model will be formulated which will attempt to predict hydrodynamic signal emanating from a small microorganism as it moves through a fluid. The strength and range of this signal (with allowances made for attenuation arising from the presence of the background turbulence which need to be taken into account over larger distances) will then be utilized to estimate the possibility that the microorganism can be perceived by a potential predator.

2 Formulation of the Encounter Rate Model

In this paper, the framework for planktonic predator prey interactions modelled as two rigid spheres moving in a viscous fluid will be formulated. These calculations will form the basis for investigations under small scale turbulence typically found in the habitat of planktonic copepods.

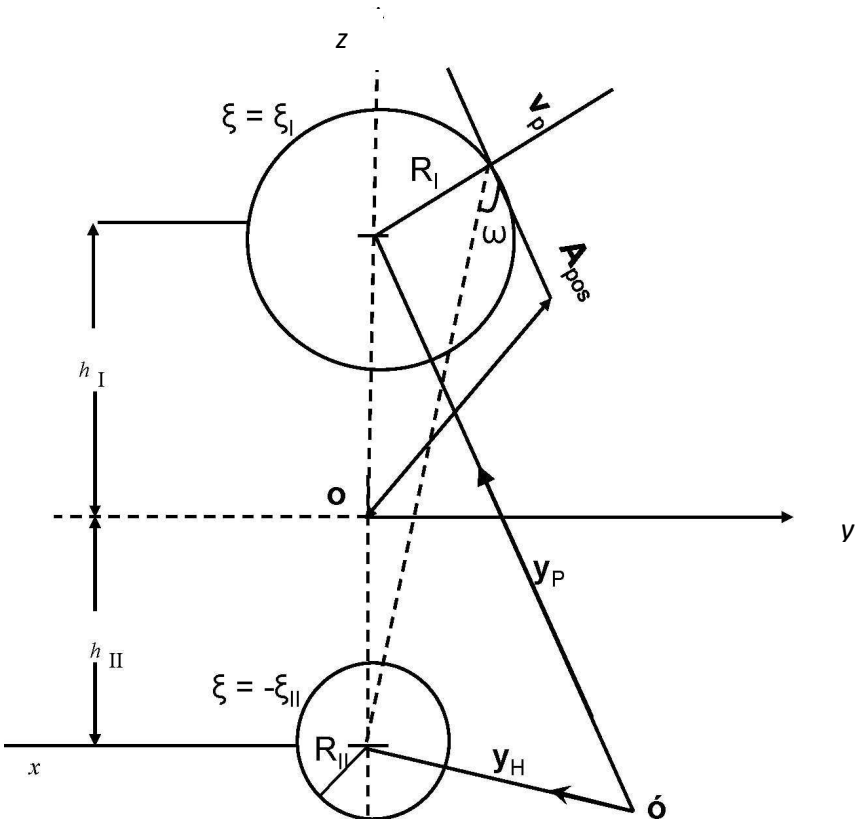

Figure 1 Geometry of the encounter situation between a predator and prey showing typical antenna position and the contact angle (ω). The contact distance is defined as $d = h_I + h_{II} - (R_I + R_{II})$, where R_I *and* R_{II} are the predator and prey sizes respectively, $\mathbf{y}_P$ *and* $\mathbf{y}_H$ are the position vectors of the of the predator and prey from some reference point **ó** respectively.

Let two planktonic microorganisms be initially positioned at a distant d apart. Geometrically this can be described as in Figure 3. The inherent bispherical nature of the problem suggests that it can best be tackled using a bispherical coordinate system (ξ,η,ϕ) in which the governing equations and the boundary conditions can be accommodated relatively easily. In terms of cylindrical coordinates (ρ,z,ϕ), the bispherical coordinates are given by Damiano2004

$$\rho = \frac{c\sin\eta}{\cosh\xi - \cos\eta}, \qquad z = \frac{c\sinh\xi}{\cosh\xi - \cos\eta}, \qquad \phi = \phi. \tag{1}$$

Here

$$0 \le \eta \le \pi, \qquad -\infty < \xi < \infty, \qquad 0 \le \phi \le 2\pi. \tag{2}$$

In this work, we shall assumed that the sphere above the plane $z = 0$ (see Figure 3) corresponds to $\xi = \xi_I$ (the predator) with radius R_I and the sphere in the lower half plane corresponds to $\xi = -\xi_{II}$ (the prey) with radius R_{II} and that both ξ_I, ξ_{II} are positive. The centre to centre separation between the two spherical bodies will be denoted by $D = h_I + h_{II}$ where $h_{I,II}^2 = R_{I,II}^2 + c^2$ (see Figure 3). We assumed further that the predator has an antennae which are situated perpendicular to its direction of motion.

2.1 Governing Equations and Solution

When considering the problem of prey perception in planktonic copepods by means hydromechanical signals in turbulent flow, the dynamic equations of the surrounding flow field around the two bodies are too complex to solve in detail. In lieu of the actual flow field, a simplified model that is valid at low Reynolds number could be adopted to estimate the signal strength in flows dominated by inertia. Even when swimming in a turbulent flow the dynamics of hydromechanical signalling is likely to be heavily influenced by the viscosity of the fluid, because over small distances (when two bodies get close together) viscosity is the determining characteristic of the background flow. So even though the global Reynolds number might be large, locally (that in the vicinity of the copepod's hydromechanical-receptors) it will be small enough to justify the application of a model based on the Stokes equations. Furthermore, the size of a sphere representing a predator used in the simulations is 3×10^{-3} m, the largest average swimming speed being 3.7×10^{-4} m s^{-1}. Thus, the Reynolds number, $R_e \approx 1.12$.

Suppose we wish to determine the velocity field in the vicinity of a planktonic predator and its prey as depicted in Figure 3. We assumed that the antenna does not alter the flow field and that the flow is sufficiently slow for the velocity field $\mathbf{v}$ to satisfy the Stokes equations

$$\mu\nabla^2\mathbf{v} = \nabla P, \tag{3}$$

$$\nabla\cdot\mathbf{v} = 0 \tag{4}$$

where μ is the dynamic viscosity of the fluid and P the pressure field. The cylindrical components of the velocity fields satisfy the form (see [13, 1])

$$v_\rho = \frac{1}{2}[(\frac{\rho}{c}\overline{W}_0^0 + W_0^1 + W_0^{-1})], \tag{5}$$

$$v_z = \frac{1}{2}[(\frac{z}{c}\overline{W}_0^0 + 2W_0^0)], \tag{6}$$

$$v_\phi = \frac{1}{2}[(W_0^{-1} - W_0^1)], \tag{7}$$

where W_0^i expressed explicitly in terms of bispherical coordinates are given by

$$W_0^i = \Delta^{\frac{1}{2}} \sum_{n=i}^{\infty} [A_{0n}^i \cosh(q\xi) + B_{0n}^i \sinh(q\xi)] P_n^i(\cos(\eta)), \tag{8}$$

$$\overline{W}_0^i = \Delta^{\frac{1}{2}} \sum_{n=i}^{\infty} [\overline{A}_{0n}^i \cosh(q\xi) + \overline{B}_{0n}^i \sinh(q\xi)] P_n^i(\cos(\eta)). \tag{9}$$

$q = \frac{2n+1}{2}$, $P_n^i(\mu)$ are associated Legendre polynomials of order n and rank i defined by

$$P_n^i(\mu) = (1-\mu^2)^{i/2} \frac{d^i}{d\mu^i} P_n(\mu) \tag{10}$$

$$\Delta = (\cosh(\xi) - \cos(\eta)). \tag{11}$$

To solve equations (3) and (3), it suffices to determine the various constants $A_{0n}^i, \overline{A}_{0n}^i, B_{0n}^i, \overline{B}_{0n}^i$ such that the equations are satisfied. These has been solved in bispherical coordinates to give a truncated infinite series. For full account of the solution see [1]. The solution is given by the system of equations (12) to ((16))

$$\begin{aligned} 0 &= 5\overline{A}_{0n}^0 - 2n\overline{A}_{0(n-1)}^0 + (n+1)\overline{A}_{0(n+1)}^0 + 2A_{0n}^{-1} - A_{0(n+1)}^{-1} - A_{0(n-1)}^{-1} \\ &- 2n(n+1)A_{0n}^1 + (n+2)(n+1)A_{0(n+1)}^1 + 2(1+2n)A_{0n}^0 \\ &- 2nA_{0(n-1)}^0 - 2(n+1)A_{0(n+1)}^0 - n(1-n)A_{0(n-1)}^1 \end{aligned} \tag{12}$$

$$\begin{aligned} 0 &= 5\overline{B}_{0n}^0 - 2n\overline{B}_{0(n-1)}^0 + (n+1)\overline{B}_{0(n+1)}^0 + 2B_{0n}^{-1} - B_{0(n+1)}^{-1} - B_{0(n-1)}^{-1} \\ &- 2n(n+1)B_{0n}^1 + (n+2)(n+1)B_{0(n+1)}^1 - 2(2n+1)B_{0n}^0 \\ &+ 2nB_{0(n-1)}^0 + 2(n+1)B_{0(n+1)}^0 - n(1-n)B_{0(n-1)}^1. \end{aligned} \tag{13}$$

$$\begin{aligned} \Lambda_n(\overline{A}_0^0, \overline{B}_0^0, \xi) &= \frac{2}{\sinh(\xi)}(\lambda_n U_z^{I,II} - \cosh(\xi)\Lambda_n(A_0^0, B_0^0, \xi) \\ &+ \frac{n\Lambda_{n-1}(A_0^0, B_0^0, \xi)}{2n-1} + \frac{(n+1)\Lambda_{n+1}(A_0^0, B_0^0, \xi)}{2n+3}), \quad n \geq 0. \end{aligned} \tag{14}$$

$$\Lambda_n(A_0^1, B_0^1, \xi) = \frac{1}{(2n-1)\sinh(\xi)}(\Lambda_{n-1}(A_0^0, B_0^0, \xi) - \lambda_{n-1} U_z^{I,II}) \tag{15}$$

$$-\frac{1}{(2n+3)\sinh(\xi)}(\Lambda_{n+1}(A_0^0, B_0^0, \xi) - \lambda_{n+1}U_z^{I,II}), \quad n \geq 1.$$

$$\Lambda_n(A_0^{-1}, B_0^{-1}, \xi) = \frac{-n(n+1)}{(2n-1)\sinh(\xi)}(\Lambda_{n-1}(A_0^0, B_0^0, \xi) - \lambda_{n-1}U_z^{I,II}) \tag{16}$$
$$+\frac{n(n+1)}{(2n+3)\sinh(\xi)}(\Lambda_{n+1}(A_0^0, B_0^0, \xi) - \lambda_{n+1}U_z^{I,II}) \quad n \geq 1.$$

Here $\Lambda_n(A,B,\xi) = A_n^i e^{\left(n+\frac{1}{2}\right)\xi} + B_n^i e^{-\left(n+\frac{1}{2}\right)\xi}$ $i = 0,-1,1$ $U_z^{I,II}$ are predator and prey speeds respectively and

$$\lambda_n = -\frac{1}{\sqrt{2}}\left(\frac{e^{-\left(n-\frac{1}{2}\right)|\xi|}}{2n-1} - \frac{e^{-\left(n+\frac{3}{2}\right)|\xi|}}{2n+3}\right).$$

By solving the system of equations (12) to (16) for the coefficients $A's$ and $B's$ the flow field in the surrounding the predator and prey is determined.

3 Kinematic Simulation

KS is a Lagrangian model that can be used to track individual particles by following their trajectories. In this method, the turbulent flow is assumed to be homogeneous and isotropic and the velocity fields are simulated using a large number of Fourier modes (see [7, 9, 10, 8, 12]). The flow fields are constructed to satisfy the incompressibility condition but it is not require to satisfy the Navier-Stokes equations . Rather, it seeks to generate flow regimes which mimic universal properties of turbulent flow on small scales without reference to any boundary condition that drive it.

One of the key parameters needed to construct KS flow fields is the rate at which the turbulent kinetic energy is dissipated into internal heat. This is commonly denoted by $\langle\varepsilon\rangle$, the $\langle\cdot\rangle$ denote ensemble average.

The flow field constructed in this paper is based on the recipe of [9]. See the paper for full account of Ks and its construction. It suffices to say here that the rate of energy dissipation rate used in this work is $\langle\varepsilon\rangle = 5.53\times10^{-9}\ \mathrm{m}^2\,\mathrm{s}^{-3}$ (see [20]).

3.1 Model setup

To formulate the encounter rate model between planktonic predator and its prey in a turbulent simulation, we shall assumed that the predator has antennae which are always aligned perpendicular to its swimming direction. We shall also assumed that the relevant hydromechanical signals are detected at the tip of one of the antennae. To set up the model, the position of the antenna will be formulated first.

Let the position vector of the prey and predator from some reference point **ó** be given by $\mathbf{y}_H$ and $\mathbf{y}_P$ respectively. This set up is depicted on Figure 3 and the antenna position ($\mathbf{A}_{pos}$) can be

defined as

$$\mathbf{A}_{pos} = h_I \hat{\mathbf{u}}_{PH} + R_I \hat{\mathbf{u}}_s + l_a \hat{\mathbf{u}}_{ant}, \tag{17}$$

where $\hat{\mathbf{u}}_{PH}$ is a unit vector, l_a is the length of the antenna and $\hat{\mathbf{u}}_{ant}$ *and* $\hat{\mathbf{u}}_s$ are unit vectors. Having specify the antenna position, the relevant signal strength at its tip can be found. The unit vector $\hat{\mathbf{u}}_{ant}$ can be defined in spherical coordinates as

$$\hat{\mathbf{u}}_{ant} = (\sin\theta\cos\phi, \sin\theta\sin\phi, \cos\theta), \tag{18}$$

where ϕ, θ are the azimuthal and zenith angles respectively. To calculate the unit vector numerically, the azimuthal angle is randomly generated. Because the antenna is perpendicular to the swimming direction, we must have $\mathbf{v}_P \cdot \hat{\mathbf{u}}_{ant} = 0$. If $\mathbf{v}_P = (v_P^x, v_P^y, v_P^z)$, then using equation (18) a relation for θ can be written as

$$\theta = \arctan\left(\frac{-v_P^z}{v_P^x\cos\phi + v_P^y\sin\phi}\right). \tag{19}$$

Now the cylindrical coordinates ρ *and* z can be written in terms of the antenna position as follows. Let $\mathbf{A}_{pos} = (A_{pos}^x, A_{pos}^y, A_{pos}^z)$. Then From equation (1)

$$\rho = \sqrt{x^2 + y^2} = \sqrt{(A_{pos}^x)^2 + (A_{pos}^y)^2} \tag{20}$$

$$z = A_{pos}^z. \tag{21}$$

Given any predator-prey separation d, the parameters c, h_I, h_{II} can now be calculated.

From equation (1) we obtained

$$\cosh\xi = \frac{\rho\cos\eta \pm c\sin\eta}{\rho}. \tag{22}$$

From equations (1) and (22) we obtained

$$\eta = \pm\arctan\left(2\frac{\rho c}{\rho^2 + z^2 - c^2}\right). \tag{23}$$

Using equation (23) the following relations are obtained

$$\sin\eta = \frac{2c\rho}{\sqrt{(c^2 - \rho^2 - z^2)^2 + 4c^2\rho^2}},$$

$$\cos\eta = \frac{(c^2 - \rho^2 - z^2)}{\sqrt{(c^2 - \rho^2 - z^2)^2 + 4c^2\rho^2}}. \tag{24}$$

Using equation (24) in (22) a formula for calculating ξ is obtained as

$$\xi = \cosh^{-1}\left(\frac{c^2(1 + 4\rho^2) - \rho^2 - z^2}{\sqrt{(c^2 - \rho^2 - z^2)^2 + 4c^2\rho^2}}\right). \tag{25}$$

3.2 Relevant hydromechanical stimuli

When a predator and prey are in close proximity, the flow-field geometries are distorted, the extent of the distortion depending upon how far they are apart. The hydrodynamic disturbances can cause a deformations of the streamlines around the antennae of the predator, which can be perceived as hydromechanical signals. Various components of the fluid disturbance can potentially serve as a mechanical cue eliciting a reaction. In this paper, the signal strength due to velocity magnitude and the rate of deformation will be considered.

The deformation rate and the velocity magnitude will be calculated using

$$\Delta = \sqrt{e_{\rho\rho}^2 + e_{\phi\phi}^2 + \frac{1}{2}e_{\rho\phi}^2 + e_{zz}^2 + \frac{1}{2}e_{\rho z}^2 + \frac{1}{2}e_{\phi z}^2}, \tag{26}$$

$$s = \sqrt{v_\rho^2 + v_z^2 + v_\phi^2}, \tag{27}$$

respectively. Here $e_{\rho\rho}$, $e_{\phi\phi}$, e_{zz}, $e_{\phi z}$, $e_{z\rho}$, and $e_{\rho\phi}$ are components of rate of stress tensor. Following [2] the signal strength s^* due to deformation can be defined by

$$s^* = l_a \Delta, \tag{28}$$

where l_a is the length scale of the antenna. In what follows, the threshold signal due to rate of deformation and velocity magnitude are respectively assumed to be 0.2 and 0.04 mm/s (see [21, 22]).

3.3 Model execution

The simulation model is similar to those of [9, 11, 8] so that only the main differences will be highlighted here. The basic simulation domain is a cube with varying sides (initial size of each side of the domain is 0.5 m). The KS flow field was constructed within the simulation domain. Initially 512 prey and predators were introduced into the domain. The same number of predators was maintained throughout. We assumed that the prey particles were non-motile phytoplankton with size 3×10^{-4} m. The second group with length scale 3×10^{-3} mm was chosen to represent the predators (see [6]). We further assume that antenna length of the template predator was 2×10^{-3} m (see [18]). The number of prey and predators introduced into the domain initially were equal (512). This fixes the prey density at a value of $512/0.5^3 \approx 4.3$ per litre a reasonable value for the pelagic marine environment. The particles were initially distributed randomly throughout the domain, with no predator in contact with any prey (all positioned at distance greater than 12 mm).

The predator particles were then assigned random walk swimming speeds drawn from three dimensional Gaussian distribution with zero mean and standard deviation σ_P, such that the collective swimming speed is $\langle v_{P,H} \rangle = \sqrt{\frac{8}{\pi}}\sigma_{P,H}$ ($\langle v_{P,H} \rangle$ are the average swimming speeds of predators and prey). This velocity in essence defines the predators'/prey direction of motion in the absence of any flow.

A predator/prey may change its swimming velocity at certain fixed intervals during the

simulation. This interval time scale is denoted by τ_{sight}. The simulation has examined two kinds of search patterns. One of which is the case where the predator never change their direction of motions throughout a run of simulation ($\tau_{sight} = \infty$). The second case predators swims by changing direction every 2.7 seconds ($\tau_{sight} = 0.2$). The prey were assumed to be non-swimming. The new innovation contained in the current model is the coupling of the two sphere model and the KS flow field.

3.3.1 Registering contacts

Deciding whether a prey in the vicinity of a predator would actually be detected by the latter (and hence registered as a 'contact') requires that the signal generated by the former which propagates to the antenna tip should exceed the appropriate detection threshold. This decision making process was done in a subroutine called Conthresh. In summary, the determination of a contact using this routine involves the following steps.

1. Using the predator and prey positions (inputs to the routine) the predator-prey separation ($d = d_1$) was calculated. This was followed by the calculation of a unit vector $\mathbf{u}_{ant}$ (see equation (18)). The angle ϕ was the generated randomly in $[0,2\pi]$ from Gaussian distribution with mean zero. This enables the calculation of the angle θ.

2. Using d_1 the parameter values $h_{I,II}, c, \xi_{I,II}$ were calculated and hence the antenna position.

3. The cylindrical coordinates ρ *and* z were then calculated from equations (20) and (21) respectively and hence ξ, η.

4. The angles ξ *and* η were then calculated from equations (25) and (23) respectively.

5. The subroutine twosphere is where the numerical evaluation of equations (12) to ((16)) were done. It returns the coefficients and importantly the signal strength s_1 to the subroutine Conthresh.

6. Steps 1 to 5 were then repeated with distance $d = d_2$ to obtain the signal s_2 (when the predator and prey are more than 12 mm apart, this constitute the background signal/noise).

7. The signal $S = | s_1 - s_2 |$ was then compared with the threshold value (Th). If $S > Th$, then CC='YES' is returned to the main routine and contact was registered otherwise no contact and CC='NO' is returned.

Whenever a contact has been designated, the angle (ω) formed by the line joining the centre of the prey to the base of the predator's antennae was measured (see Figure 5). This is called the contact angle. Similarly, the distance (along the line of centres) between the surfaces of the predator and prey was also measured. This is called the contact distance.

4 Results and Discussion

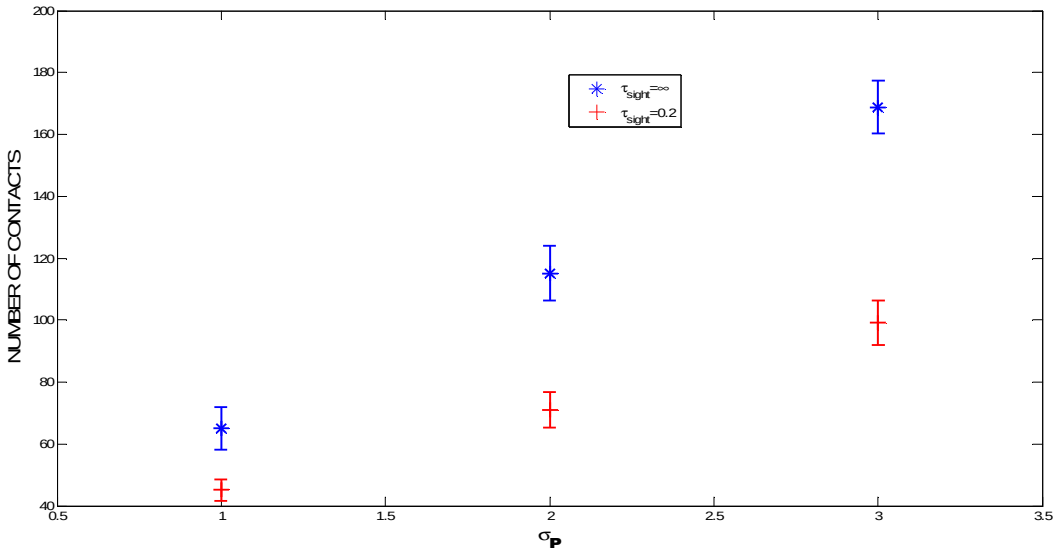

(a)

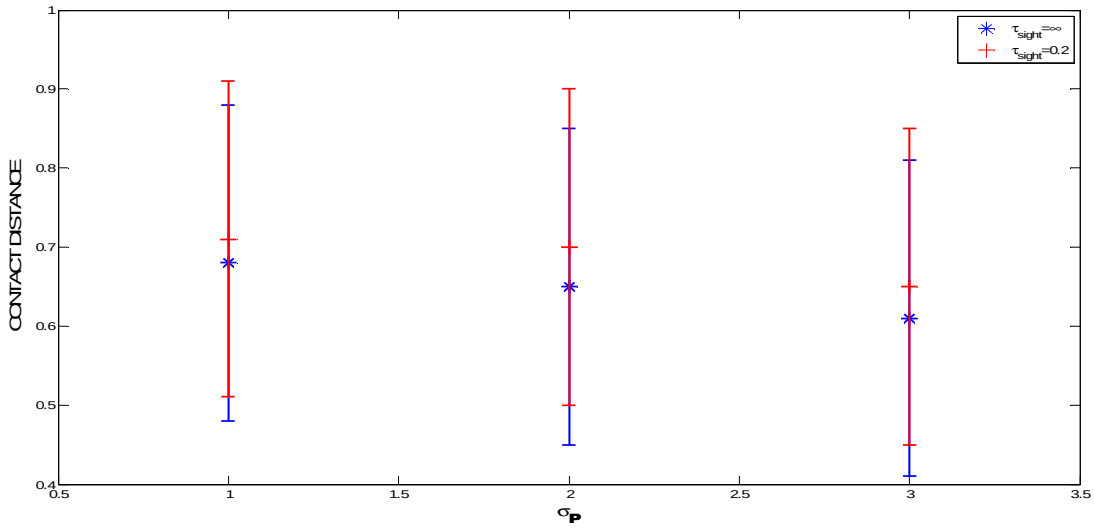

(b)

Figure 2: Number of contacts, average contact distances, recorded for 2 groups of 512 predators against the swimming speeds for a signal based on the differences between velocity magnitudes. (a) Depicts the number of contacts for straight line swimmers (*, $\tau_{sight} = \infty$) and random walk swimmers (+, $\tau_{sight} = 0.2$). (b) Depicts the average contact distances recorded during the simulation against the predators' swimming speeds. The contact distances are the separation between the predator and prey on contact.

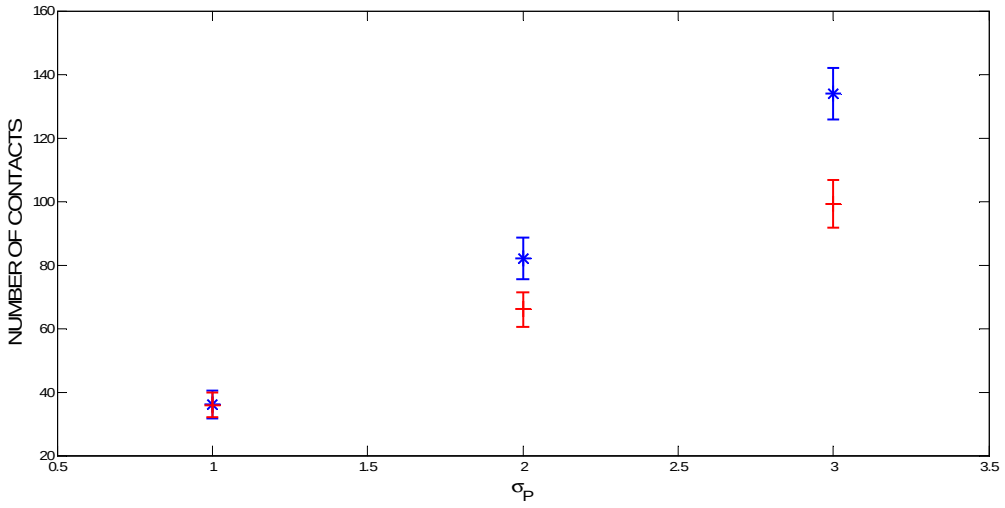
NUMBER OF CONTACTS
160
140
120
100
80
60
40
20
0.5
1
1.5
2
2.5
3
3.5
σP

walk swim do not differ significantly. As σ_P increases, the trajectories of the predators undergoing random walk become more and more convoluted as more time was spent re-tracking the same volume of fluid (see [19]). Hence, the divergence of contact rate for the two motility patterns.

Figures 2(b) and 3(b) show the average contact distances against the variances of swimming speed. Comparison of the two Figures also shows that the average contact distances do not differ so much when the different types of flow signal are employed. When swimming randomly predators can perceive prey at marginally greater distances than when they swim in straight lines.

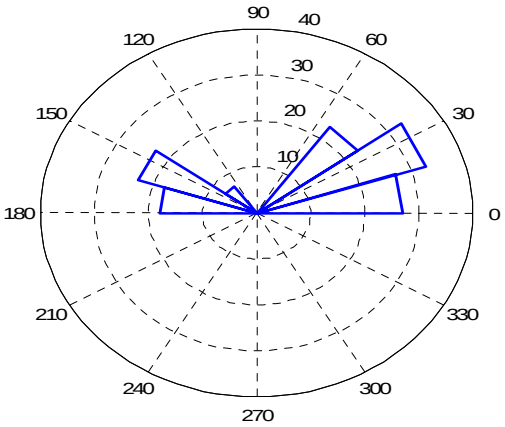

(a)

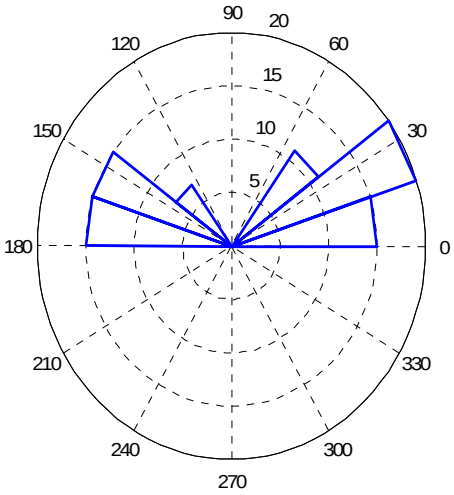

(b)

Figure 4: Frequency histogram for contact angles arising from signals due to velocity magnitude in one run of simulations. These results are obtained by recording the angle ω (see Figure 6) whenever contact occur between a predator and prey and using them to form the frequency histogram. (a) Depicts the results for the straight line swimmers (b) Shows the results for the random walk swimmers

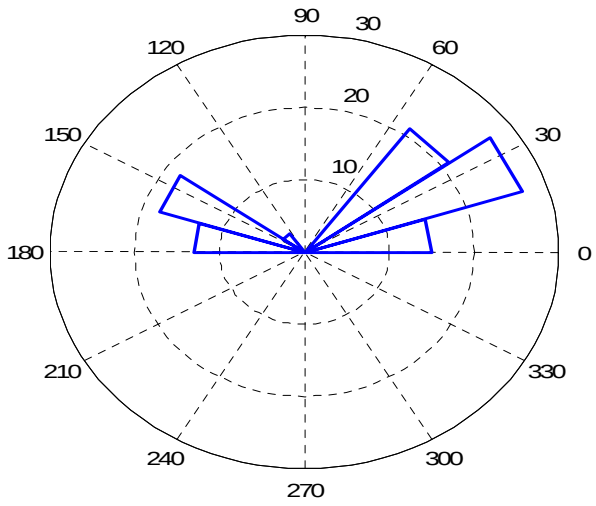

(a)

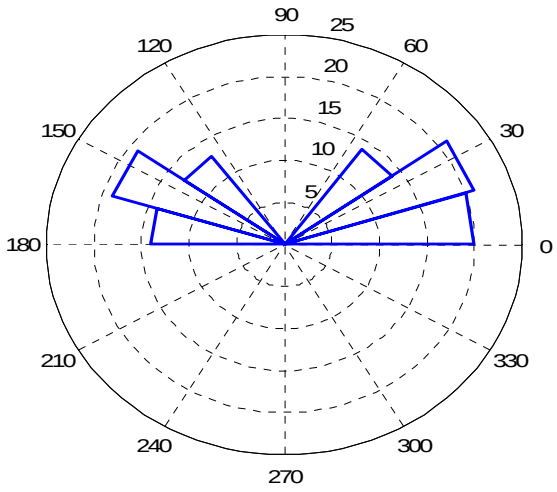

(b)

Figure 5: Frequency histogram for contact angles arising from signal strength due to rate of deformation, in one run of simulations. Other keys are the same as in Figure 5. (a) Depicts the results for the straight line swimmers (b) Shows the results for the random walk swimmers

Whenever any contact was designated to have occurred, the contact angle (see Figures 1 and 6) was recorded. When the antenna is perpendicular to the line of centres and the predator is moving in the direction of decreasing $z, \omega = 0$. The angles were used to form a frequency

histogram as shown on Figures 4 and 5. These further serve to illustrate that planktonic particles perceived their prey at a range of different orientations. When a predator and prey approaches each other head on, the angle ω is defined to be 0^o. In all the Figures, more contacts were recorded in the range $[20,\ 40^o]$ than any other relative orientation. Note that no contacts were recorded at 90^o. As the relative orientation $\rightarrow 90^o$ from either direction, the antennae moved further away from the scene of disturbance (see Figure 6).

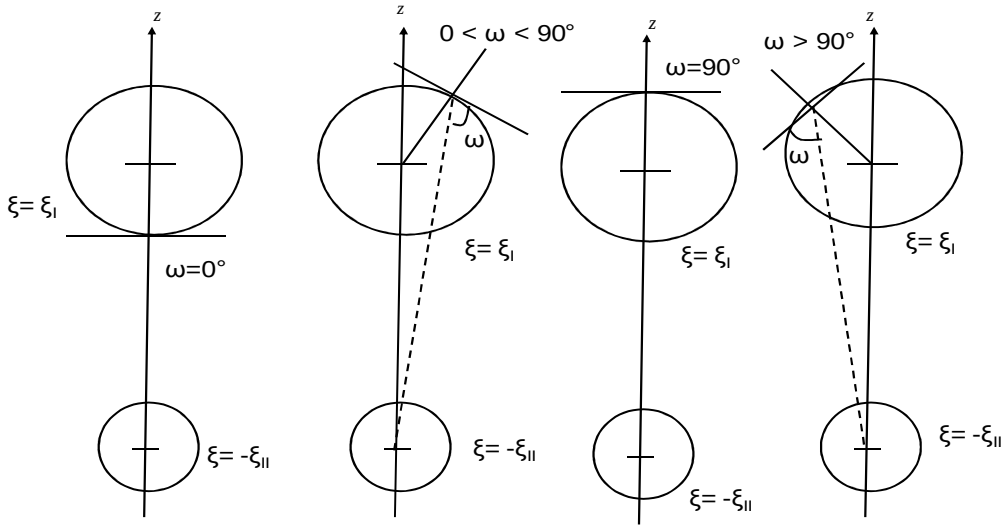

Figure 6: Schematic diagram showing some possible range of the contact angle ω which depend on the position of the antenna. When the antenna is perpendicular to the line of centres and the predator is moving in the direction of decreasing $z, \omega = 0$. However, when the antenna is perpendicular to the line of centres and the predator is moving in the direction of increasing $z, \omega = 90^o$.

One observation that we can make from these results is that the number of contacts drops off to zero in the range $[60,\ 120^o]$. This does not necessarily means that contacts cannot occur in those orientations. It is merely indicates that the net signals generated were not sufficient to rise above the threshold.

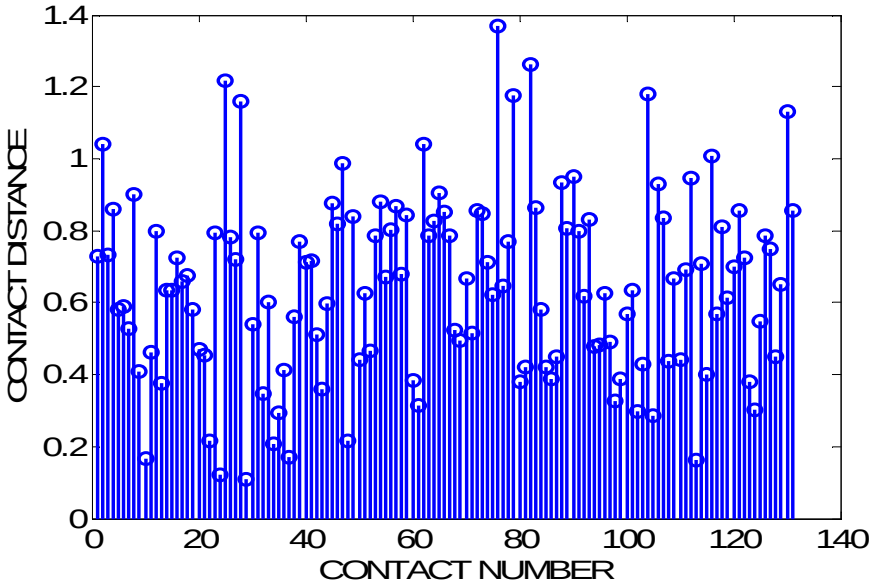

(a)

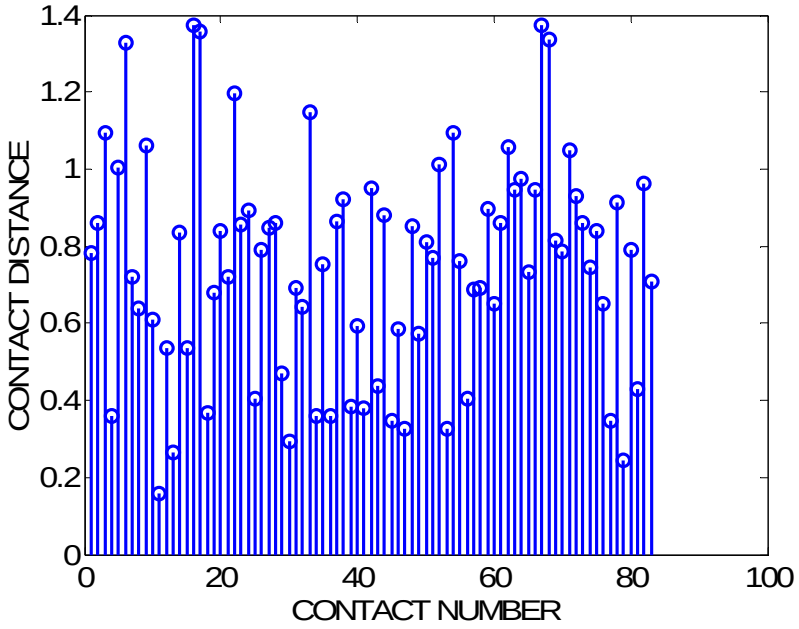

(b)

Figure 7: Stem plot for contact distance against the contact number. For example, the first contact in (a) occurred at a distance of 0.76 approximately. This is for signal strength due to velocity magnitude, in one set of the simulations. (a) Is for straight line swimmers while (b) is for random walk swimmers.

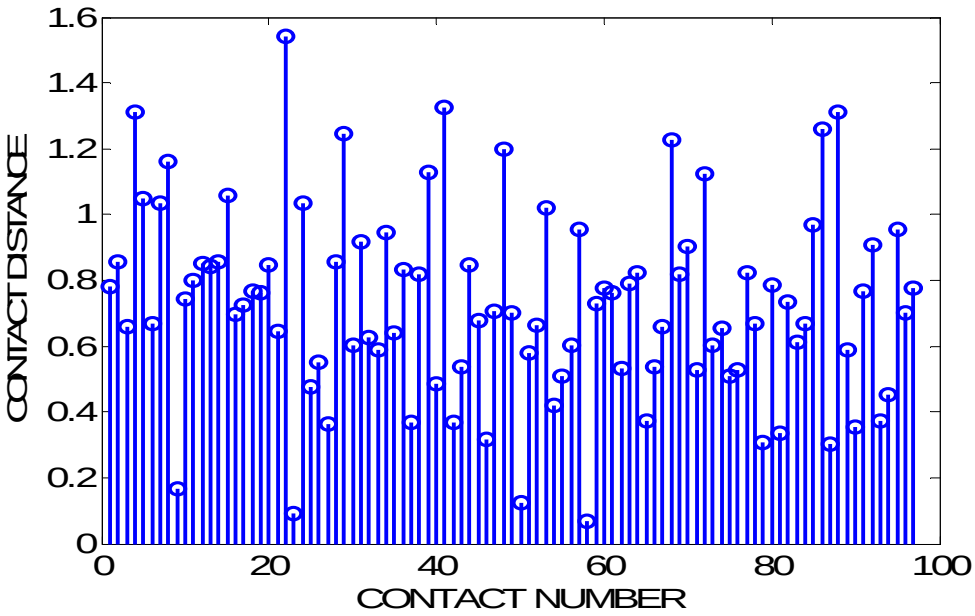

(a)

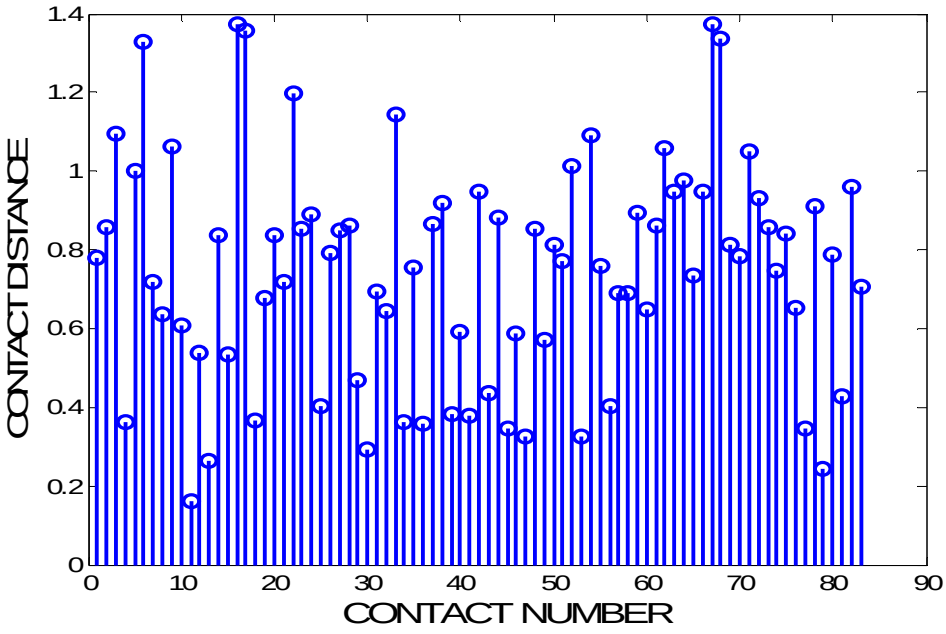

(b)

Figure 8: Stem plot for contact distance against the contact number. For example, the first contact in (a) occurred at a distance of 0.8 approximately. This is for signal strength due to deformation rate, in one run of simulations. (a) Is for straight line swimmers while (b) is for random walk swimmers.

Figures 7 and 8 shows the stem plot illustrating the range of distances at which prey particles were perceived for the two different motility patterns during one run of simulation. The results were obtained by recording the first contact and the distance at which it occurred, the second contact and the distance at which it occurred and so on. The large variation across the distances suggest the existence of large error bars. The variations of the distances occur due to the differences in the strength of the signal as predator and prey move towards each other. Small distances are associated with low signals. When the signal strength is very high, the predator can detect the presence of the prey some considerable distance away. The averages of these distances over 10 runs of simulations at various speeds are depicted in Figures 2(b) and 3(b).

5 Conclusion

In this paper, encounter rates for predators perceiving prey by hydromechanical signals in a turbulent flow were studied. The model framework for determining the signal generated by a small prey microorganism in the vicinity of a predator was constructed by employing methods originally designed to study the classical problem of two spheres of arbitrary sizes and speeds falling in Stokes flow. Extensions to the classical problem were made by adding sensory structures (antennae) to one of the spheres (predator). The new setting was then introduced into a small scale turbulent flow. The rate at which a group of such predators encounter their prey was then investigated using two forms of signal modalities. The main conclusions are as follows:

1. The contact radius of a typical planktonic predator is not a fix constant. Predators can perceive prey over wide range of separation distances. This is in complete contrast to predators with spherically symmetric perception field, where, prey are perceived at an identical distance in all orientations.
2. Prey perception tend to occur when the relative orientation between the predator and prey were in the range $[20,\ 40^{o}.]$
3. Predators swimming by changing directions tend to perceives prey marginally further away than those swimming constantly in straight lines.
4. Predators can perceive prey over wide range of separation distances.
5. In almost all encounter rates studies in literature the perception field of planktonic predators is automatically assumed to be spherical. Here, more evidence were presented that the perception field of predators perceiving prey by hydromechanical signals is not spherical.
6. The final conclusion is that predators perceiving prey by hydromechanical means are more sensitive to signals due to velocity magnitude than the deformation rates counterparts.

References

[1] Bala, Saminu Iliyasu. On the hydrodynamic interactions between two spheres in Stokes flow. *African Scientist*, To appear, 2010.

[2] Caparroy, Philippe and Thygesen, Uffe H. and Visser, Andre W. Modelling the attack success of planktonic

predators: patterns and mechanism of prey selectivity. *Journal of Plankton Research*, 22(10):1871-1900, 2000.
[3] Fields, D. M. and Yen, J. The escape behavior of marine copepods in response to a quantifiable fluid mechanical disturbance. *Journal of Plankton Research*, 19:1289-1304, 1997.
[4] Galbraith, Peter S. and Browman, Howard I. and Racca, Roberto G. and Skftesvik, Anne Berit and Saint-Pierre, Jean-Francois. Effect of turbulence on the energetics of foraging in Atlantic cod Gadus morhua larvae. *Marine Ecology Progress Series*, 281:241-257, 2004.
[5] Gerritsen,J. and Strickler, J. R. Encounter probabilities and community structure in zooplankton: a mathematical model. *J. Fish Res. Board Can.*, 34:73-82, 1977.
[6] Greene, C. H. Foraging tactics and prey-selection patterns of omnivorous and carnivorous calanoid copepods. *Hydrobiologia*, 167/168:295-302, 1988.
[7] Kraichnan, Robert H. Diffusion by a Random Velocity Field. *The Physics of Fluids*, 13(1):22-31, 1970.
[8] Lewis, D. M. and Bala, Saminu. Iliyasu. Plankton predation rates in turbulence: A study of the limitations imposed on a predator with a non-spherical field of sensory perception. *Journal of Theoretical Biology*, 242:44-61, 2006.
[9] Lewis, D. M. and Pedley, T. J. Planktonic contact rates in homogeneous isotropic turbulence: theoretical predictions and kinematics simulations. *J. Theor. Biol.*, 205:377-408, 2000.
[10] Lewis, D. M. and Pedley, T. J. The influence of turbulence on plankton predation strategies. *J.Theor. Biol.*, 210:347-365, 2001.
[11] Lewis, D.M. Planktonic contact rates in in homogeneous isotropic turbulence: case of predator with limited sensory field of perception. *J.Theor.Biol.*, 234:73-97, 2003.
[12] Lewis, David Mark and Bala, Saminu Iliyasu. An examination of sal fee strategies employed by fish larvae foraging in a variety of different turbulent regimes. *Mar Ecol Prog Ser*, 359:261-274, 2008.
[13] Lin, C. J. and Lee, K. J. and Sather, N. F. Slow motion of two spheres in a shear field. *J. Fluid Mech.*, 43:35-47, 1970.
[14] Rothschild, B. J. and Osborn, T. R. Small-scale turbulence and plankton contact rates. *J. Plankton Res.*, 10:465-474, 1988.
[15] Ki%rboe , T. and Saiz, E. Planktivorous feeding in calm and turbulent environments with emphasis on copepods. *Mar. Ecol. Prog. Ser*, 122:135-145, 1995.
[16] Ki%rboe , T. and Saiz, E. and Visser, A. W. Hydrodynamic signal perception in the copopod Acartia tonsa. *Mar. Ecol. Prog. Ser*, 179:97-111, 1999.
[17] Ki%rboe , T. and Visser, A. W. Predator perception in copepods due to hydromechanical signals. *Mar. Ecol. Prog. Ser.*, 179:81-95, 1999.
[18] Visser, Andre W. Hydromechanical signals in plankton. *Mar. Ecol. Prog. Ser.*, 222:1-24, 2001.
[19] Visser, Andre W. and Ki%rboe , Thomas. Plankton motility pattern and encounter rates. *Oecologia*, 148:538-546, 2006.
[20] amazaki, H. and Osborn, T. R. and Squires, K. D. Direct Numerical simulation of planktonic contact rate in turbulent flow. *J. Plankton Res.*, 10:629-643, 1991.
[21] Yen, J. and Lenz, J.H. and Gassie, J.J.V. and Hartline, J.J.K. Mechanoreception in marine copepods: Electrophysiological studies on the first antennae. *J. Plankton Res.*, 14:495-512, 1992.
[22] Yen, Jeannette and Sanderson, Brian and Strickler, J. R and Akubo A. Feeding Currents and Energy Dissipation by Eucheta rimana, a Subtropical Pelagic Copepod. *Limnology and Oceanography*, 16(2):538-546, 1991.